JOURNAL OF VIROLOGY, July 2009, p. 6599–6609 Vol. 83, No. 13
0022-538X/09/$08.00+0 doi:10.1128/JVI.01819-08

Role of Microtubules in Extracellular Release of Poliovirus▽†

Matthew P. Taylor,[1]‡ Trever B. Burgon,[1] Karla Kirkegaard,[1]* and William T. Jackson[2]

Department of Microbiology and Immunology, Stanford University School of Medicine, Stanford, California,[1] and Department of Microbiology and Molecular Genetics, Medical College of Wisconsin, Milwaukee, Wisconsin[2]

Received 29 August 2008/Accepted 3 April 2009

Cellular autophagy, a process that directs cytosolic contents to the endosomal and lysosomal pathways via the formation of double-membraned vesicles, is a crucial aspect of innate immunity to many intracellular pathogens. However, evidence is accumulating that certain RNA viruses, such as poliovirus, subvert this pathway to facilitate viral growth. The autophagosome-like membranes induced during infection with wild-type poliovirus were found to be, unlike cellular autophagosomes, relatively immobile. Their mobility increased upon nocodazole treatment, arguing that vesicular tethering is microtubule dependent. In cells infected with a mutant virus that is defective in its interaction with the host cytoskeleton and secretory pathway, vesicle movement increased, indicating reduced tethering. In all cases, the release of tethering correlated with increased amounts of extracellular virus, which is consistent with the hypothesis that small amounts of cytosol and virus entrapped by double-membraned structures could be released via fusion with the plasma membrane. We propose that this extracellular delivery of cytoplasmic contents be termed autophagosome-mediated exit without lysis (AWOL). This pathway could explain the observed exit, in the apparent absence of cellular lysis, of other cytoplasmic macromolecular complexes, including infectious agents and complexes of aggregated proteins.

Infection with lytic viruses, by definition, leads to the destruction of host cells. In fact, lysis often has been assumed to be the only mechanism by which nonenveloped viruses can exit infected cells, because usually they do not have access to the lumen of the host secretory pathway. Nevertheless, nonenveloped viruses have been observed in the extracellular milieu in the apparent absence of cell lysis. For example, hepatitis A virus, a small nonenveloped RNA virus of the *Picornaviridae*, can establish persistent infections with no visible cytopathic effect, yet it has been observed to spread from cell to cell in tissue culture and in infected liver (21) (reviewed in reference 24). Poliovirus, also a picornavirus, can lyse cells in tissue culture and in infected animals. However, it also may be able to spread nonlytically: persistent infections of tissue culture cells have been reported to be associated with abundant poliovirus in the cell medium (41, 45, 46). The interpretation of all of these experiments is plagued by the possibility that the lysis of a very few cells could go undetected yet lead to the presence of substantial virus in the extracellular medium. Some experimental support for a nonlytic cellular exit route for poliovirus has come from studies of infected polarized monolayers of Caco2 cells. Even when there was no apparent breach in the monolayer, based upon the maintenance of electrical resistance, progeny virions were observed in the medium facing the apical, but not the basolateral, surface of the intact monolayer (65). Similar findings were reported for simian virus 40, a double-stranded DNA virus that assembles in the nuclei of infected cells (13). These observations suggest that virus can be released nonlytically from the apical cell surfaces.

What kinds of processes in infected cells could give rise to nonlytic exit? Infection is known to lead to dramatic changes in the morphology and physiology of host cells visible by light and electron microscopy, classically termed the cytopathic effect. Within 3 to 4 h, cells infected with poliovirus accumulate large numbers of membranous vesicles (8). Although the topology and origin of these membranes have been debated, the original micrographs of Dales et al. (14) and ultrastructural analysis performed by high-pressure cryofixation and freeze substitution to preserve membrane morphology (22, 54, 58) have shown that poliovirus-induced vesicles predominately are double-membraned structures with cytoplasmic contents. Single-membraned vesicles could be induced in mammalian cells and in *Saccharomyces cerevisiae* by the expression of poliovirus proteins 2C and 2BC in isolation (3, 12, 63), whereas both viral proteins 2BC and 3A were required to induce the formation of double-membraned vesicles (58). By 5 or 6 h, several hours before the lysis of most cells, infected cells begin to lose attachment to the substratum, and the cellular microtubule and intermediate filament networks collapse (17, 39). The cytoskeletal alterations are dramatic (29); curiously, however, cytoskeletal integrity was found to have no effect on the intracellular yield of poliovirus (16).

The double-membraned vesicles that accumulate during poliovirus infection resemble, in many respects, double-membraned cellular autophagosomes, which envelop cytosolic contents to target them for autophagic degradation (reviewed in references 31, 34, 40, and 44). Poliovirus-induced vesicles, like autophagosomes, contain lipidated cellular protein LC3 and the late endosomal protein LAMP-1 (27, 58, 61). The reduc-

* Corresponding author. Mailing address: Department of Microbiology and Immunology, Fairchild Science Building D309A, Stanford University School of Medicine, Stanford, CA 94305-5402. Phone: (650) 498-7075. Fax: (650) 498-7147. E-mail: karlak@stanford.edu.

† Supplemental material for this article may be found at http://jvi.asm.org/.

‡ Present address: Department of Molecular Biology, Princeton University, Princeton, NJ 08544.

▽ Published ahead of print on 15 April 2009.

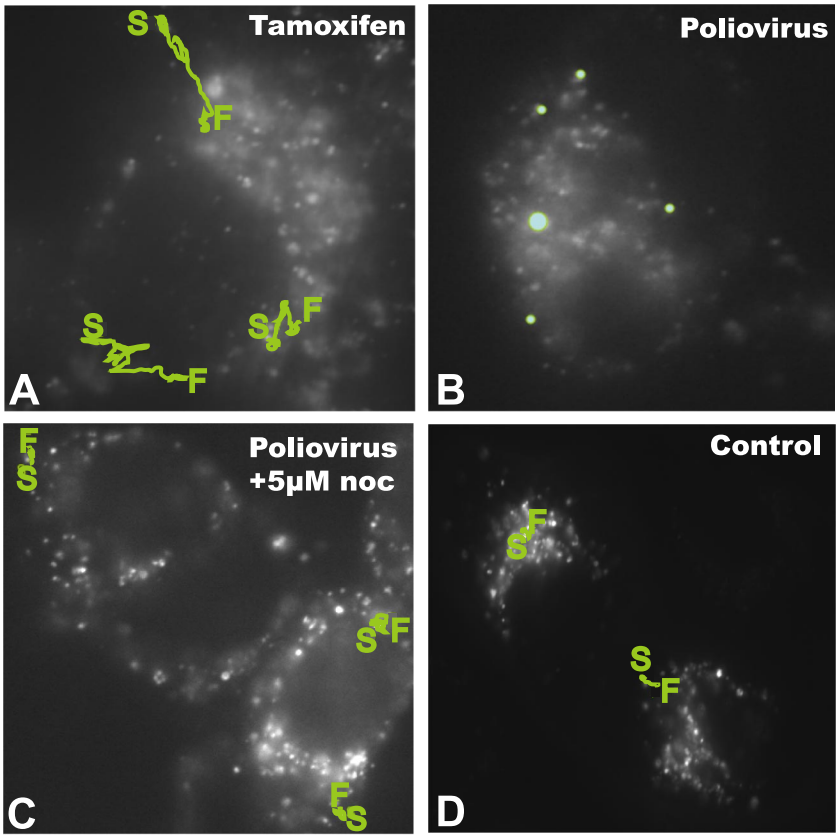

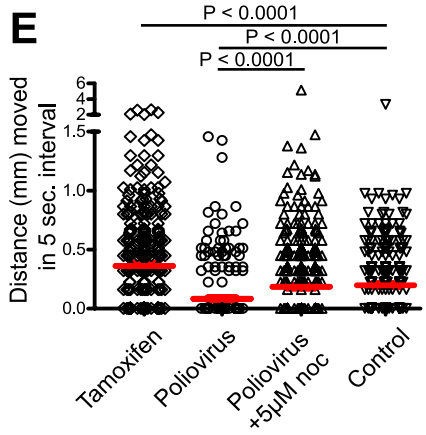

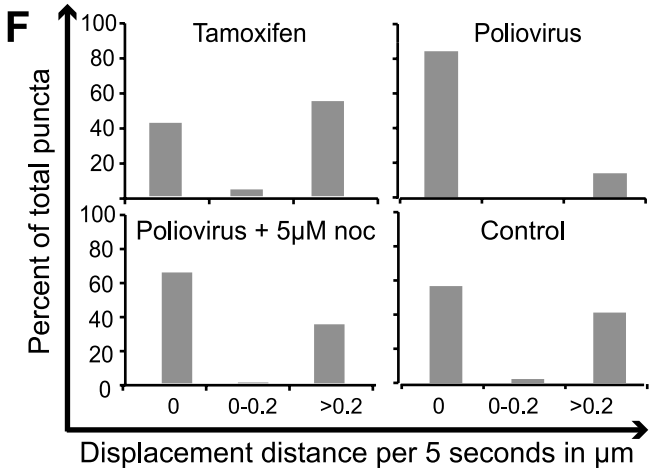

tion of the amounts of autophagy proteins Atg12 and LC3 via RNA interference treatment led to a decrease in the yield of intracellular virus (27), supporting the idea that components of the autophagy pathway are subverted by poliovirus to benefit viral growth. Prompted by the finding that the reduction of autophagy proteins LC3 and Atg12 decreased the amount of extracellular virus even more than intracellular virus (27), we have suggested that the viruses within the cytoplasmic lumena of double-membraned vesicles are released into the extracellular milieu (27, 33, 62). Here, we provide evidence that the association of virus-induced vesicles with the microtubule network can modulate the extracellular release of poliovirus. These findings strengthen the argument that the autophagosomal constituents contribute to the nonlytic viral release and reveal a potential pathway for its control.

MATERIALS AND METHODS

Cells and viruses. Human H1 HeLa cells were cultured as monolayers in Eagle's minimum essential medium (E-MEM) supplemented with 10% (vol/vol) calf serum, 100 U of penicillin/ml, and 100 U of streptomycin/ml at 37°C and 5% CO_2. Poliovirus type 1 Mahoney and 3A-2 (7) viruses were propagated from an infectious cDNA plasmid (47), as has been previously described (15).

Plasmids and transfections. The green fluorescent protein (GFP)-LC3 expression plasmid used here has been described previously (27). Transfections were carried out using Effectene (Qiagen) according to the manufacturer's instructions. GFP-LC3 was assayed 1 to 2 days posttransfection.

Viral infections and drug treatments. Infections were performed as described previously in 60-mm tissue culture dishes (27). For extracellular analysis, viruses were absorbed to cells for 30 min in phosphate-buffered saline (PBS) containing $MgCl_2$ and $CaCl_2$, washed twice in medium, and then refed with 4 ml of medium. For extracellular virus, aliquots of medium were collected at appropriate time points, any floating cells were collected by centrifugation for 3 min at $1,000 \times g$, and supernatants were analyzed by plaque assay. For intracellular virus, cells were scraped into 1 ml of PBS supplemented with 1 mM each calcium and magnesium chloride and lysed by freeze-thaw, whereupon cytoplasmic extracts were prepared by centrifugation. Tamoxifen and nocodazole (Sigma) were dissolved in 1:1 dimethylsulfoxide (DMSO)-ethanol and added to cells in fresh medium. The mock-treated controls were treated with equivalent volumes of 1:1 DMSO-ethanol and received similar medium changes and washing treatments. Tamoxifen treatments were for 48 h at a final concentration of 10 μM and were continued through the infection. Nocodazole was added at final concentrations of 5 or 15 μM, as indicated, immediately following viral absorption. Both concentrations of nocodazole caused the complete disruption of microtubule networks, as visualized by immunofluorescence (data not shown).

Cell viability staining. Cells were harvested by scraping, washed with PBS, and resuspended in 1 ml PBS. Cells then were stained for 30 min with 1 ml Live/Dead reagent (Invitrogen, Carlsbad, CA) at 4°C. Following staining, cells were washed, fixed in freshly made 4% paraformaldehyde, and analyzed on a FACScan flow cytometer (Becton Dickinson).

Microscopy and immunofluorescence. For live imaging, H1 HeLa cells were grown in 8-well LabTek coverslides (NUNC) in E-MEM supplemented with 0.2 M HEPES. Transfection with GFP-LC3 plasmid was performed with Effectene (Qiagen) according to the manufacturer's directions, and cells were observed 48 h after transfection. Images were captured every 5 s for a 5-min period on a Zeiss Axiovert 200 M microscope with Openlab 5.0.1 software. Cells for microtubule staining were fixed in 20°C methanol for at least 5 min. A monoclonal murine antibody to α-tubulin (T-9026; Sigma) was used at a 1:100 dilution in PBS-BT (PBS with 3% bovine serum albumin and 0.1% Triton X-100) for 30 min at room temperature. Cells were washed three times in PBS-BT, and anti-mouse secondary antibody (SC-2084; Santa Cruz) was added at a 1:250 dilution. Cells were washed again in PBS-BT and stained in 4′,6′-diamidino-2-phenylindole (DAPI; 100 ng/ml in PBS) for 2 min. Cells were washed again and mounted under Vectashield (Vector Labs) and imaged on a Zeiss Axiovert 200 M microscope with Openlab 5.0.1 software.

Quantitation of movement. The movement of GFP-LC3 puncta was quantified manually by measuring the displacement of individual punctum from sequential frames taken every 5 s. Distances were quantified using the Openlab software and calibrated using a stage micrometer. The distances between displaced puncta were measured only when an obvious and unique spot of similar morphology could be identified after the 5-s interval; if puncta appeared or disappeared between frames, they were not quantified. Measurements were made from the point closest to the relative center of each punctum. For each experiment, a minimum of 200 spots was quantified to achieve the median plotted values. Calculation of significance values was done using a one-way analysis of variance or a pairwise *t* test analysis provided by GraphPad Prism 5.0 software.

RESULTS

Movement of poliovirus-induced vesicles in live infected cells is restricted by the microtubule network. To investigate whether poliovirus-induced vesicles, like autophagosomes, move within cells by a microtubule-dependent mechanism, we compared the mobility of bona fide autophagosomes induced by tamoxifen, an inducer of autophagy (10), to that of poliovirus-induced vesicles. To identify autophagosomal structures, H1 HeLa cells were transfected with a plasmid that encodes GFP-LC3. LC3 originally was identified as being microtubule associated and, in the absence of lipidation or autophagy induction, is localized in the cytosol. Upon the induction of autophagy, however, LC3 is a specific marker of autophagosomes, recruited to double-membraned vesicles from its cytoplasmic location via the addition of phosphatidylethanolamine to its C terminus (25, 60). As shown in Fig. 1A, numerous bright spots of GFP-LC3 fluorescence can be seen in H1 HeLa cells treated with tamoxifen to induce autophagy. These punctate, GFP-LC3-containing structures were highly motile. Typical trajectories are shown by green tracings, with the locations of starting and finishing indicated for those puncta that could be followed during a 5-min period. Hundreds of other randomly chosen 5-s displacement measurements from the same cells are plotted in Fig. 1E and F. Approximately 60% of bona fide autophagosomes (Fig. 1A) were found to display movement during any given 5-s interval (Fig. 1F), with a median displacement of 0.36 μm (Fig. 1E). The observed displacements can be seen more dramatically when viewed as movies (see the supplemental material) and confirm previous reports of autophagosomal movement induced by starvation or rapamycin (18, 28, 32, 35).

In cells infected with poliovirus, the GFP-LC3-containing puncta were surprisingly motionless. Figure 1B shows tracings

FIG. 1. Movement of GFP-LC3 puncta. HeLa cells transfected with a GFP-LC3 expression plasmid were visualized after (A) 48 h of treatment with 10 μM tamoxifen, delivered in a small volume of a 1:1 mixture of DMSO and ethanol, the solvent for both tamoxifen and nocodazole (noc); (B) 5 h after infection with poliovirus at a multiplicity of infection of 50 PFU/cell in the presence of the solvent; and (C) 5 h after infection with poliovirus in the presence of 5 μM nocodazole. (D) An uninfected control in the presence of the solvent. S, starting point; F, finishing point. Individual GFP-LC3 puncta that could be identified during the course of the entire 5-min imaging period were tracked, and their course is highlighted in green. Movies were made of each set of cells, with images taken every 5 s for 5 min (see the supplemental material). (E) Quantitation of the displacement of 200 individual puncta for the first 25 s of each movie was performed and is plotted; median displacements are shown in red. (F) The data from panel E are plotted in a different way to show the distribution of movement distances for individual puncta from each treatment.

of randomly selected puncta during the 5-min observation period. More than 80% of the puncta observed showed no detectable displacement (Fig. 1F). The median displacement of 200 different puncta was 0.03 μm per 5-s interval (Fig. 1E). This immobility was somewhat relieved by treatment with 5 μM nocodazole (Fig. 1C), which increased the median displacement observed per 5-s interval sixfold, to 0.18 μm (Fig. 1E), and increased the percentage of motile GFP-LC3-containing structures from 10 to 30%. Figure 1D shows the movement and localization of GFP-LC3 in mock-treated H1 HeLa cells. This pattern also was slightly punctate, although these puncta were less numerous and less bright than those observed during autophagy or poliovirus infection. It has been shown previously by us and others that LC3-GFP puncta in untreated cells do not colocalize with LAMP-1 or correlate with LC3 lipidation (2, 27), and presumably they represent cytoplasmic aggregates. In any case, the mobility of these GFP-LC3-containing structures (a median of 0.19 μm per 5-s interval) was considerably reduced from that of bona fide autophagosomes (Fig. 1A) and considerably increased from that of the puncta in poliovirus-infected cells (Fig. 1B). We conclude that the GFP-LC3-containing membranes in poliovirus-infected cells are immobilized relative to either cellular autophagosomes or cytoplasmic constituents, and this immobilization is due to direct tethering to microtubules or is dependent on microtubule integrity via indirect means.

Nocodazole treatment increases extracellular virus release by a mechanism that does not correlate with toxicity. We have surmised that the double-membraned topology of poliovirus-induced vesicles can promote the nonlytic release of this nonenveloped, nominally lytic virus by entrapping cytosolic poliovirions within their lumena late in infection (27, 33). The relative immobility of the poliovirus-induced vesicles (Fig. 1) thus came as a surprise and suggested the possibility that microtubule integrity regulates the nonlytic release of such membrane-trapped virions. To test this hypothesis, we performed a time course to monitor the accumulation of extracellular virus in the absence and presence of 5 μM nocodazole. As shown in Fig. 2A, very little extracellular virus was observed as late as 4.5 h postinfection either in the absence or presence of nocodazole. However, by 6 h postinfection, a fivefold increase in extracellular virus was observed in cells treated with nocodazole, while mock-treated infected cells showed no increase in the yield of extracellular virus.

The presence of increased amounts of extracellular virus at 6 h postinfection, a time point much earlier than the expected lysis of infected cells, could have resulted from the increased nonlytic release of small amounts of virus from many cells or from the premature lysis of a few infected cells. To test whether the enhanced amount of extracellular virus in the presence of 5 μM nocodazole correlated with any cytotoxicity, we analyzed the intracellular and extracellular yield of poliovirus in the absence and presence of nocodazole at a higher nocodazole concentration. The presence of either 5 or 15 μM nocodazole did not significantly affect the amount of intracellular virus (Fig. 2B). However, large increases in the amount of extracellular virus were observed in the presence of both 5 and 15 μM nocodazole (Fig. 2C). To test whether these concentrations of nocodazole increased the amount of cell death in infected cells, a fluorescent dye that stains only cells with permeabilized membranes (Live/Dead; Invitrogen) was used to monitor cell viability by flow cytometry. The treatment of cells with the DMSO-ethanol solvent control solution did not affect cell viability (Fig. 2D). Neither of two nocodazole concentrations affected the viability of infected (Fig. 2E) or uninfected (Table 1) cells. Therefore, the increased extracellular yield of poliovirus in the presence of nocodazole (Fig. 2A, C) did not correlate with observable cell toxicity or death.

Changes in microtubule distribution during infection with wild-type and 3A-2 mutant poliovirus. Alterations in cytoskeletal morphology during poliovirus infection have been documented for decades (17, 29, 39). Changes in the structure of the microtubule network in poliovirus-infected cells can be seen through the use of an antibody directed against tubulin. During wild-type infection, the morphology of the microtubule network remained indistinguishable from that of uninfected cells until 9 h postinfection, at which time most infected cells displayed a ring of collapsed microtubules encircling the nucleus. The mechanism for this late loss of microtubule integrity is not known.

The only poliovirus protein that has been reported to have any direct interaction with the cytoskeleton is nonstructural protein 3A (36). Two-hybrid experiments have revealed a number of potential cellular-interacting partners for this 87-amino-acid protein, including LIS-1, a component of the dynactin complex involved in dynein-dependent motion along microtubules (36). The nuclear magnetic resonance structure of the soluble, amino-terminal 59 amino acids of 3A protein (57), missing only the hydrophobic region near its carboxyl terminus that is required for membrane association (64), is shown in Fig. 3A. Residues 20 to 57 were shown to form two α-helices that engage in dimeric contacts, while the 19 amino-terminal residues of each monomer were found to be natively unstructured (57). The addition of a single Ser residue between amino acids 12 and 13 of poliovirus 3A protein yields a mutant virus known as 3A-2 (7). At 37°C, the conditions of these experiments, only a slight growth defect was observed for the 3A-2 mutant virus relative to the growth of the wild-type virus. Nevertheless, altered interactions with host cells were seen in which neither the pronounced inhibition of host protein secretion displayed by wild-type virus (15) nor the physical interaction with GBF-1, a host protein known to be involved in protein traffic (5), was observed.

To determine whether the microtubule collapse observed for wild-type poliovirus-infected cells was similar in cells infected with 3A-2 mutant virus, parallel infections were examined at identical time points (Fig. 3B). In mutant virus-infected cells, microtubule collapse was observed 2 h earlier than that in wild-type virus-infected cells, at 7 instead of 9 h postinfection. These data suggest either that a wild-type function of 3A protein that is defective in the 3A-2 mutant virus actively stabilizes microtubules during poliovirus infection, or that the mutant infection creates a more destabilizing environment.

Nocodazole-enhanced release of extracellular virus release is bypassed during infection with 3A-2 mutant virus. To explore any further effects of the 3A-2 virus mutation on microtubule function during poliovirus infection, we investigated the early release of extracellular virus from cells infected with 3A-2 mutant poliovirus. As in wild-type virus-infected cells, little extracellular virus was observed until 6 h postinfection. How-

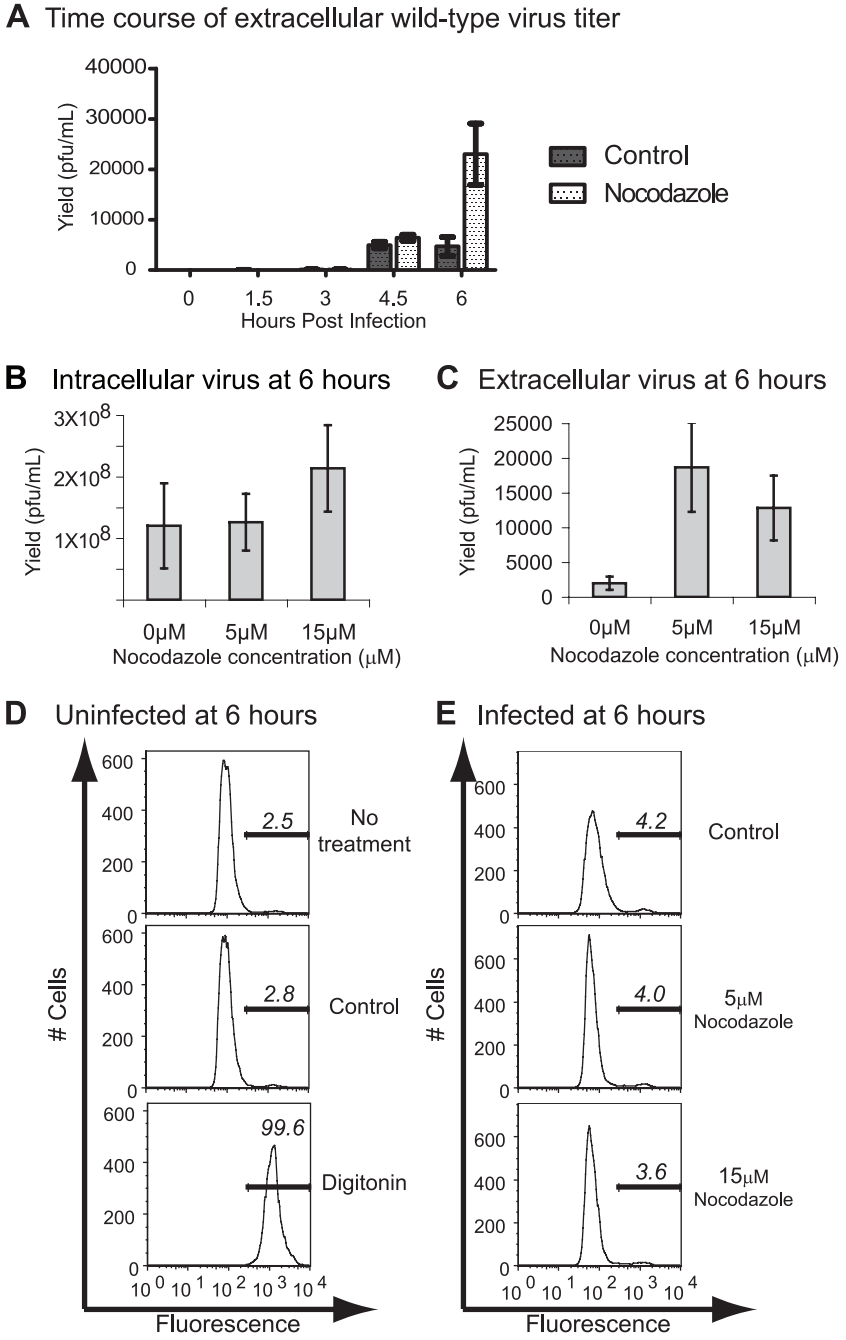

FIG. 2. Extracellular release of poliovirus. HeLa cells were infected with wild-type poliovirus (multiplicity of infection, 0.1 PFU/cell) and either mock treated or treated with nocodazole at the concentrations indicated. (A) A time course of poliovirus extracellular titers in the presence or absence of 5 μM nocodazole; the volume of medium per experiment was 4 ml. In an independent set of experiments, titers of intracellular (B) and extracellular (C) viruses from infected cells at two different nocodazole concentrations are shown. Mean and standard errors from triplicate experiments are provided; extracellular virus was collected in 4 ml of medium, and intracellular virus stocks were prepared in 1 ml PBS. (D) Analysis by flow cytometry indicates the viability of uninfected cells upon treatment with a DMSO-ethanol solvent solution and upon treatment with digitonin. Bars in each plot represent the percentage of dead cells present. (E) Cells infected with wild-type poliovirus (multiplicity of infection, 10 PFU/cell) and mock treated (control) or treated with 5 or 15 μm nocodazole were analyzed for viability. These and similar data are summarized in Table 1.

ever, unlike wild-type virus-infected cells, the amount of extracellular virus observed in 3A-2 virus-infected cells was not affected by treatment with 5 μM nocodazole (Fig. 4A). This effect can be seen in direct comparison to data for wild-type virus in Fig. 4B, in which the increase in extracellular virus upon treatment with 5 mM nocodazole for wild-type, but not 3A-2 mutant, virus infections can be seen readily. The increase in extracellular 3A-2 virus relative to the growth of the wild-

TABLE 1. Viability of HeLa cells that were uninfected or infected with the indicated virus in the presence and absence of nocodazole[a]

Infection status	Time postinfection (h)	Treatment	% Inviable cells
Uninfected*	6*	Untreated	2.5
		DMSO-ethanol	2.8
		Digitonin	99.6
Wild type*	6*	DMSO-ethanol	4.2
		5 μM nocodazole	4.0
		15 μM nocodazole	3.6
	8	DMSO-ethanol	5.4
		5 μM nocodazole	4.0
		15 μM nocodazole	3.5
3A-2 mutant	6	DMSO-ethanol	5.0
		5 μM nocodazole	4.3
		15 μM nocodazole	4.4
	8	DMSO-ethanol	4.7
		5 μM nocodazole	4.0
		15 μM nocodazole	3.6

[a] The percentage of inviable cells was determined by fluorescence-activated cell sorting after the incubation of cells with Live/Dead stain to assay plasma membrane permeability (Invitrogen, Carlsbad, CA). Asterisks indicate data for which fluorescence-activated cell sorting plots are shown in Fig. 2.

type virus in the absence of nocodazole is especially surprising, given that the intracellular yield of 3A-2 mutant virus was reduced compared to that of wild-type virus (Fig. 4C). Time courses of infection with both wild-type and 3A-2 viruses, performed in both the absence and the presence of nocodazole, showed no differences in the amount of cell death between 3A-2 virus-infected and wild-type virus-infected cells, or in the presence or absence of nocodazole, at any given time postinfection (Table 1). This argues that the increase in extracellular virus during 3A-2 virus infection and during the treatment of wild-type virus-infected cells with nocodazole was not due to increased cell death. Therefore, the increase in extracellular virus and the nocodazole independence of that extracellular virus in 3A-2 mutant virus-infected cells might reflect the altered cell biology of infection by mutant and wild-type viruses.

Mobility of membranous vesicles induced during 3A-2 mutant virus infection. To test whether the microtubule-dependent tethering of GFP-LC3-containing membranes was altered in cells infected with 3A-2 mutant poliovirus, we compared the mobility of these structures in wild-type and mutant virus-infected cells at 5 h postinfection, a time point immediately preceding the increase in extracellular virus observed in 3A-2 virus-infected cultures (Fig. 4A). Representative trajectories of GFP-LC3-containing puncta in wild-type and 3A-2 virus-infected cells are displayed in Fig. 5A and B. Figure 5C shows the quantitation of the movies that are available in the supplemental material. In these movies, GFP-LC3-containing puncta were found, as in Fig. 1, to be nearly immobile in wild-type poliovirus-infected cells, displaying median displacements of only 0.03 μm per 5-s interval. However, most of the GFP-LC3-containing vesicles in 3A-2 virus-infected cells were highly motile, with median distances of 0.32 μm per 5-s interval (Fig. 5 C, D), which are comparable to the displacements shown by GFP-LC3-containing structures upon tamoxifen treatment (Fig. 1). This finding further strengthens the observed correlation between the release of the microtubule-dependent tethering of

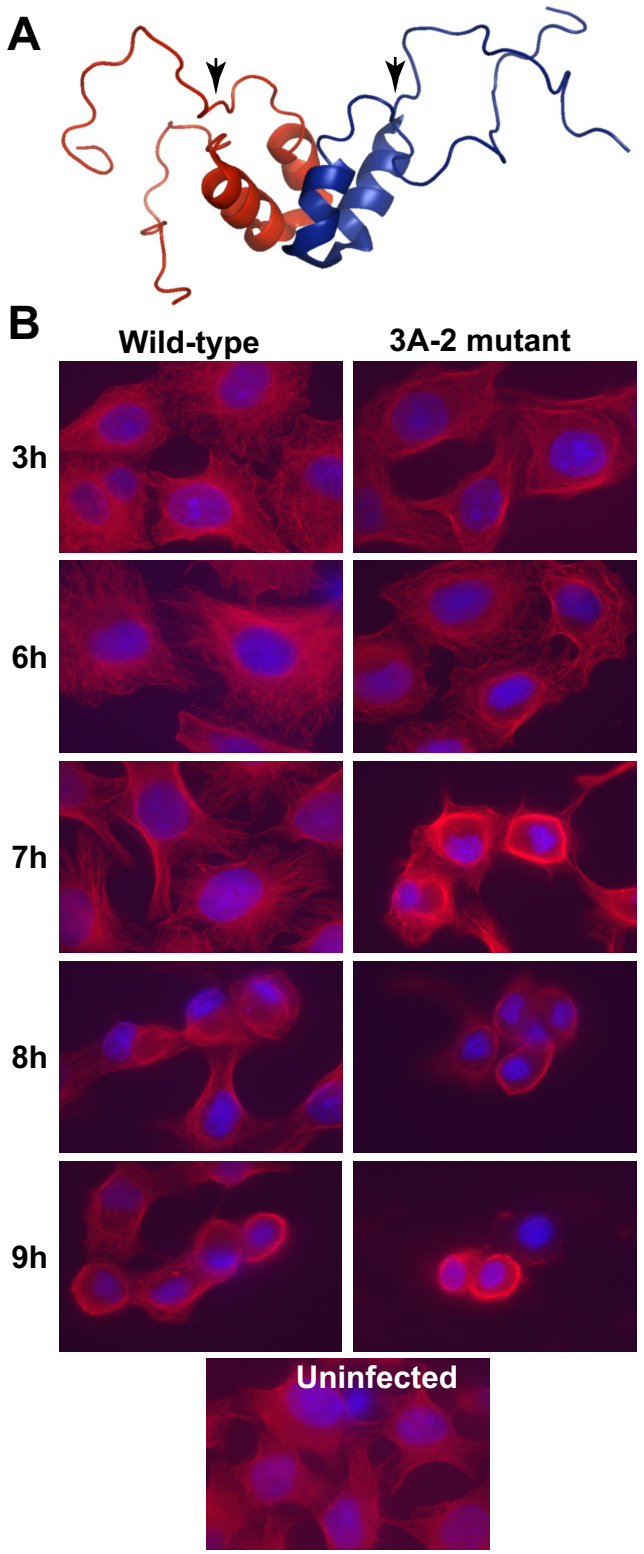

FIG. 3. Integrity of the microtubule network in cells infected with wild-type and 3A-2 mutant poliovirus. (A) Ribbon model of the homodimeric structure of the 59 N-terminal residues of poliovirus protein 3A (39). Arrowheads indicate the positions of the Ser insertion mutation of the 3A-2 mutant virus. (B) HeLa cells were infected with wild-type or 3A-2 mutant poliovirus (multiplicity of infection, 50 PFU/cell) and fixed at the indicated times postinfection. Microtubules (red) were visualized with indirect immunofluorescence using anti-tubulin antibody. Nuclei (52) were stained with DAPI.

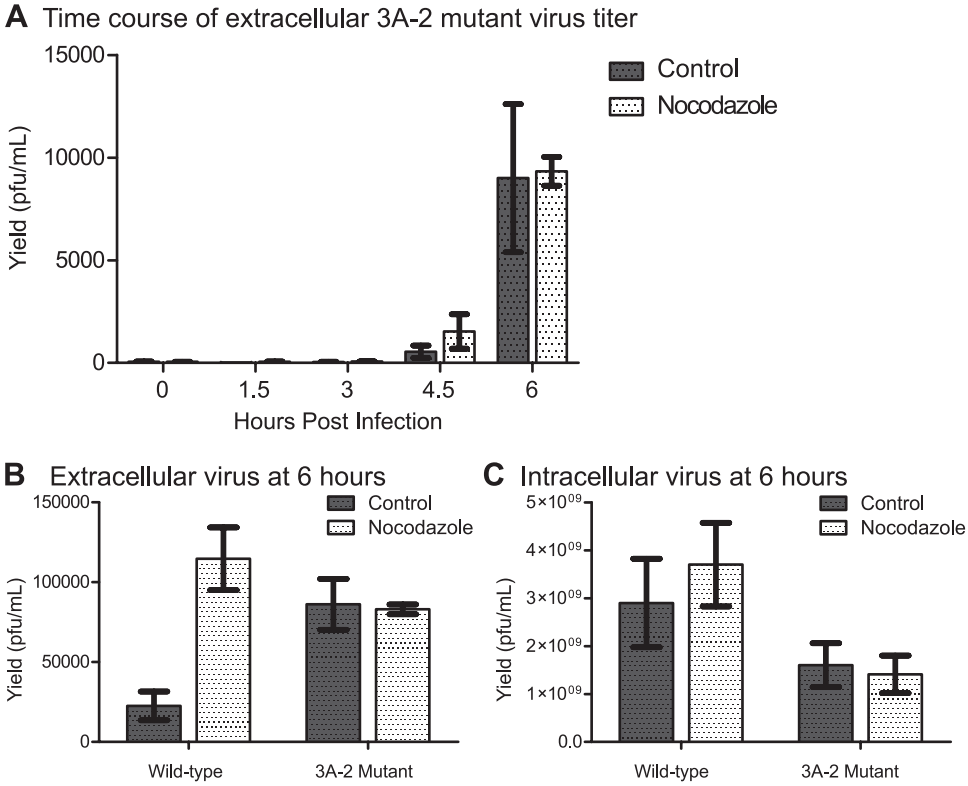

FIG. 4. Extracellular release of 3A-2 mutant poliovirus. HeLa cells were infected as described in the legend to Fig. 2 with wild-type and 3A-2 mutant viruses. (A) A time course of the amounts of 3A-2 extracellular virus in the medium of infected cells cultured in the presence or absence of 5 μM nocodazole. In independent experiments, the titers of intracellular (B) or extracellular (C) virus from cells infected with wild-type and 3A-2 mutant viruses in the presence and absence of 5 μM nocodazole as indicated are shown. Mean values and standard errors from triplicate experiments are provided.

GFP-LC3-containing vesicles formed during poliovirus infection and the extracellular release of infectious virus.

DISCUSSION

Poliovirus-induced membranous vesicles and cellular autophagosomes are similar in several respects, including their double-membraned topology, cytoplasmic lumena, and decoration by LAMP1 and lipidated LC3. In this paper, we describe another similarity: their association with cellular microtubules. Bona fide autophagosomes traffic in an anterograde direction along the microtubule network using cytoplasmic dynein as a motor, promoting their fusion with lysosomes and subsequent maturation into autolysosomes. In addition, the microinjection of antibodies directed against LC3 results in the immobilization of autophagosomes via microtubule attachment (32). This is not entirely surprising, as LC3 originally was identified as a microtubule-associated protein (37). Several enveloped viruses, especially those that infect neurons such as pseudorabies virus (19, 42), traffic in a retrograde direction along microtubules to facilitate cell exit by budding (48, 56). In contrast, we found that poliovirus-induced vesicles are nearly immobilized within infected cells by a mechanism dependent on the integrity of microtubules and the wild-type function of viral protein 3A. Although the mechanism for this attachment is not yet known, viral protein 3A is known to bind directly to LIS1 (36), a component of the dynein/dynactin complex whose abundance affects dynein motor function and microtubule network morphology (55).

Previously, we demonstrated that the integrity of the autophagy pathway is beneficial for poliovirus replication, and autophagy pathway function correlates with a disproportionately large increase in extracellular poliovirus as early as 5 to 6 h after infection (27). Therefore, we suggested that the double-membraned topology of autophagosome-like vesicles facilitated the extracellular, nonlytic release of cytosolic contents such as poliovirus particles. Here, we have shown that poliovirus-induced vesicles are nearly immobilized during infection. The destruction of the integrity of the microtubule network with nocodazole increased the mobility of poliovirus-induced vesicles and, concomitantly, the amount of extracellular virus. Infection with a mutant virus, 3A-2, which contains a single-amino-acid insertion in its natively unstructured N-terminal domain, also increased both the mobility of the LC3-containing membranes and the amount of extracellular virus released. Interestingly, the median mobilities of the GFP-LC3-containing puncta in wild-type poliovirus-infected cells in the presence of nocodazole (Fig. 1) and in 3A-2 virus-infected cells (Fig. 5) are very similar, strengthening the argument that both of these GFP-LC3-containing structures were moving independently of microtubules. That the amount of extracellular 3A-2 virus released was insensitive to nocodazole also supports the hypothesis that the wild-type function of 3A protein is required to

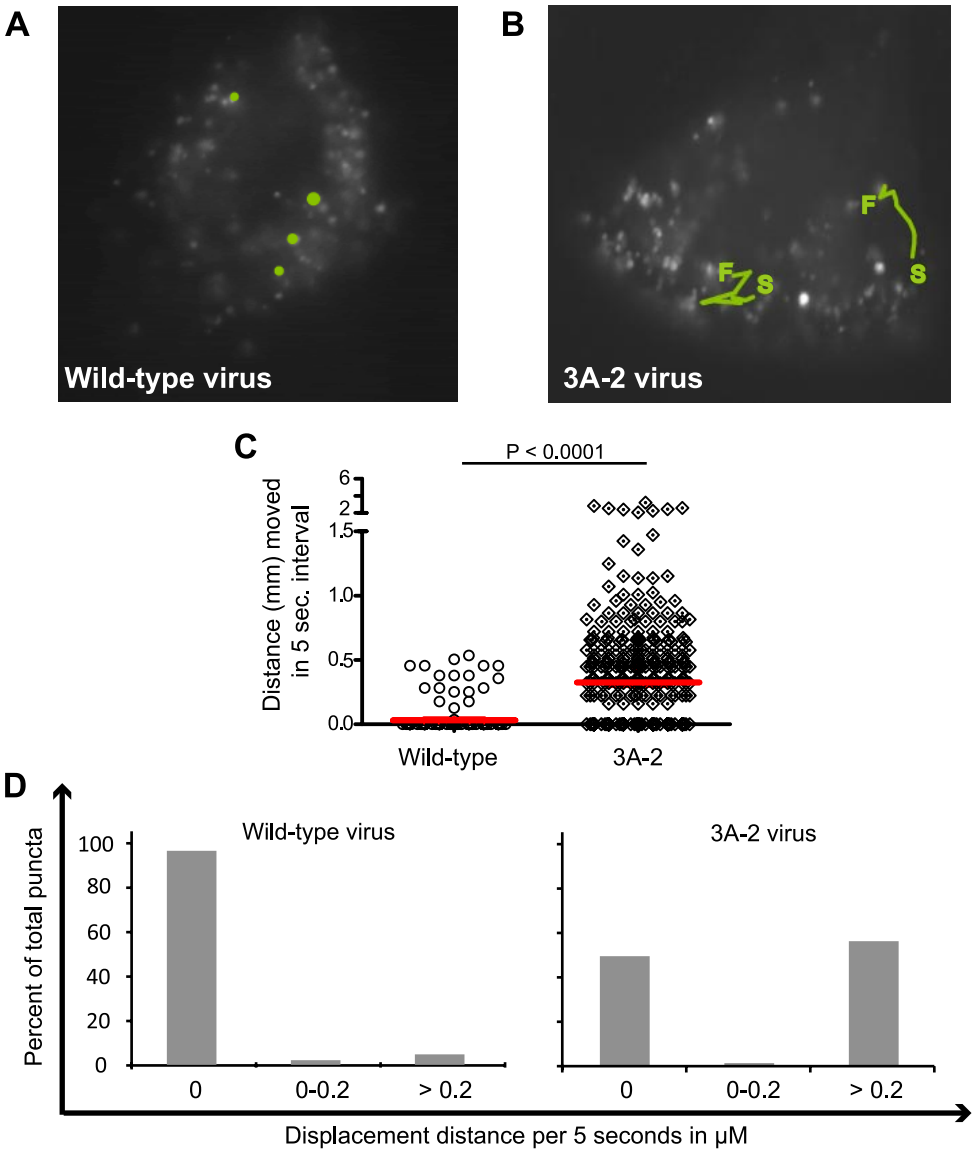

FIG. 5. Movement of GFP-LC3 puncta during infection with wild-type and 3A-2 mutant poliovirus. HeLa cells transfected with GFP-LC3 expression plasmid were visualized after 5 h of infection with wild-type (A) or 3A-2 mutant (B) poliovirus at a multiplicity of infection of 50 PFU/cell. S, starting point; F, finishing point. Movies were prepared in which images taken every 5 s of a 5-min time course were compiled (see the supplemental material). Several puncta that could be monitored during the 5-min period were tracked and are highlighted in green. (C) Quantitation of the movements of hundreds of puncta over 5-s intervals for the first 25 s of each movie was determined, and median values are plotted. (D) The data from panel C are displayed to show the distribution of movement distances.

tether the poliovirus-induced vesicles to intact microtubules. We propose that the nonlytic escape of cytoplasmic constituents is facilitated by the unusual double-membraned topology of autophagosome-like membranes and is controlled by their microtubule-binding properties. We further propose that this novel pathway be termed autophagosome-mediated exit without lysis (AWOL) (Fig. 6).

For any instance of the release of cytoplasmic material in the absence of apparent cell lysis, it is difficult to determine whether the release resulted from the lysis of a few cells or the leakage of many cells. The inspection of the cytoplasmic contents of the double-membraned vesicles induced by poliovirus between 4.5 and 6 h postinfection (14, 54) reveals that as many as one-third of the hundreds of virus-induced double-membraned vesicles in each cell contained a few virions in the entrapped cytosol. We need to explain the presence of approximately 10^4 infectious virus particles in the extracellular milieu (Fig. 2A). If these were released by the lysis of a few cells, given that each infected HeLa cell harbors from 100 to 1,000 infectious virions under these conditions (W. Jackson, data not shown), from 10 to 100 cells would have to have lysed. In contrast, if all of the extracellular virus was leaked from the 100,000 cells on the plate by AWOL, assuming a particle/PFU ratio of 100, then each cell would have, on average, leaked very few particles, approximately 10 virus particles per cell. In the presence of nocodazole, the 75,000 infectious virus particles

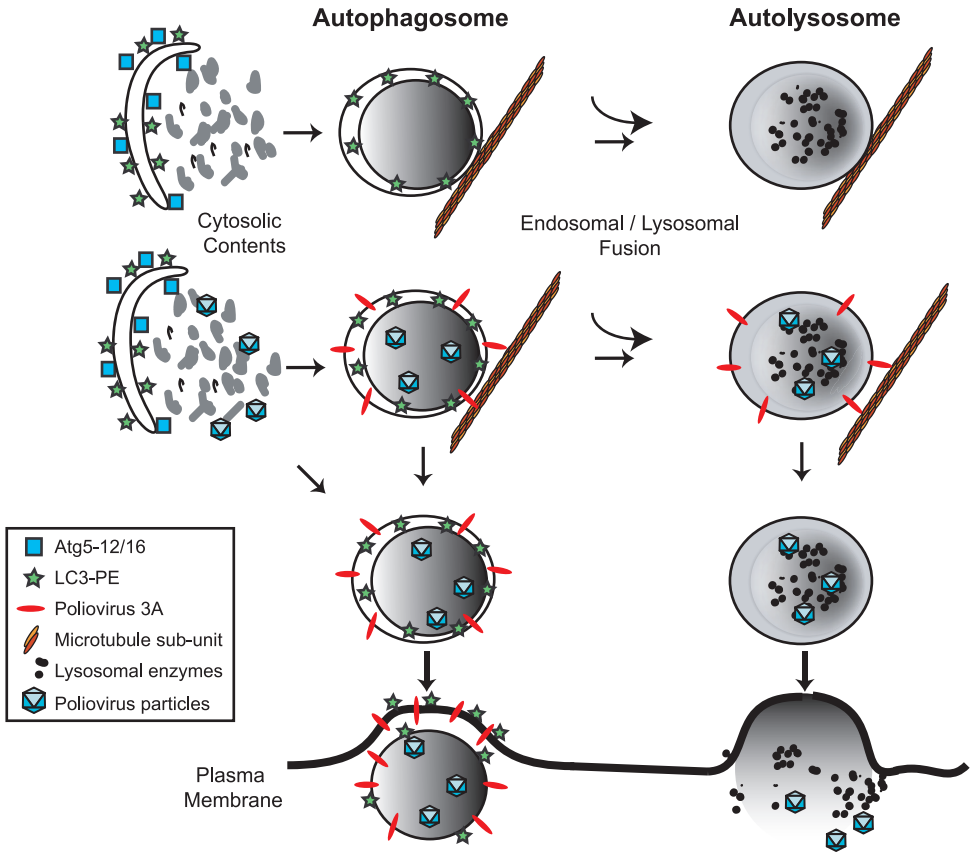

FIG. 6. AWOL. Autophagosome-like membranes formed during viral infection can interact with viral particles in different ways. Early in infection, the cytosol enveloped by the double membranes is not likely to contain infectious virions. Later in infection, however, newly formed double-membraned vesicles may or may not contain virions in the cytoplasmic lumen. The viral 3A protein is shown in red and is meant to represent all of the viral proteins in the RNA replication complex. In cells infected with wild-type poliovirus, the virally induced vesicles are tethered to microtubules by a mechanism that is dependent on the wild-type function of viral protein 3A; whether or not this contact is direct is not known. We propose that the occasional fusion of autophagosome-like vesicles with the plasma membrane is not favored by this tethering, which can be disrupted either by depolymerizing microtubules or by the 3A-2 mutation in the 3A protein. Finally, the hypothesized release of virus in the lumenal compartment can occur either before or after fusion with endosomal or lysosomal organelles, which then will cause the release of either membrane-enclosed or free virus.

released (Fig. 2A) would correspond to the leakage of 70 particles per cell. Thus, to provide a significant amount of extracellular cytoplasmic material, events of fusion between double-membraned vesicles and the plasma membrane would not need to be frequent.

In this study, several lines of evidence indicated that the extracellular virus observed during poliovirus infection did not derive exclusively from lysed cells. As the concentration of nocodazole increased from 5 to 15 μM, the release of virus did not increase. In addition, infection with 3A-2 mutant virus yielded consistently more extracellular virus than wild-type virus. Neither nocodazole treatment nor 3A-2 virus infection increased the amount of measurable cell death over that observed in wild-type poliovirus infection. Finally, if the increase in extracellular virus in 3A-2 mutant virus-infected and in nocodazole-treated cells both resulted from increased cell lysis, one would expect these cytotoxic effects to be additive. Instead, nocodazole treatment had no effect on the amount of extracellular 3A-2 mutant virus, arguing that these two perturbations affect the same pathway.

The release of cytosolic material by mechanisms that do not involve the canonical secretory pathway or apparent cell lysis has been most convincingly argued for Theiler's virus (53) but also has been suggested for hepatitis A virus, simian virus 40, rotavirus, *Cryptococcus neoformans*, and aggregated α-synuclein and huntingtin proteins (1, 4, 21, 30, 38, 51). In many of these cases, autophagomes or autophagy-related proteins have been found in the vicinity of the enigmatically released material. Specifically, proteins that are prone to aggregation, such as α-synuclein, tau, and huntingtin, are found frequently within autophagosomes, and autophagy is crucial for the clearance of such aggregates (23, 26, 49, 50, 66). The cytoplasmic membranes associated with poliovirus RNA replication contain both LAMP-1 and LC3 (27), those associated with rotavirus particle formation contain LC-3 (6), and the membranes that surround maturing *Cryptococcus neoformans* before cell egress contain LAMP-1 (1).

While aggregated proteins or even *Cryptococcus* cells might be targeted to the cytoplasmic lumen of an autophagosome, it is more difficult to explain how intact poliovirions are found there. The membranous vesicles induced during poliovirus infection have been shown by many elegant studies from the

laboratory of Kurt Bienz (University of Basel) to bear, on their cytoplasmic surfaces, all of the protein constituents of the poliovirus RNA replication complex as well as newly synthesized poliovirus negative- and positive-sense RNA strands (8, 9, 11). Therefore, it would be expected that newly synthesized virions are found free in the cytoplasm of infected cells. This is, in fact, the location of most viral progeny, which can become so concentrated as to form crystalline arrays within the cytosol; however, small numbers of viral particles also have been observed within the cytoplasmic lumena of double-membraned vesicles (14, 27, 54). The most parsimonious explanation of this surprising topology is that double-membraned vesicles that form late in infection can sequester cytosol that contains virions (Fig. 6).

One of the most interesting aspects of cellular autophagosomes is their unusual topology: having enveloped the cytosol, they accumulate degradative enzymes via fusion with vesicles from the endocytic and lysosomal pathways. Lipases and protease are thought to degrade the inner of the two membranes, whereupon the double-membraned autophagosome matures to the single-membraned autolysosome (reviewed in reference 43). This event accomplishes the topological conversion of cytosol to lumen. As depicted in Fig. 6, the exit of cytosolic contents by AWOL could occur from the fusion of single-membraned autolysosome-type vesicles, releasing the formerly cytoplasmic constituents directly into the extracellular milieu, or from the fusion of double-membraned autophagosome-type membranes, which could release cytoplasmic contents in small packets enclosed by a single membrane likely to be unstable outside the cell. For poliovirus, we do not yet know the physical state of the membranes involved in the postulated nonlytic release of virus. Double-membraned vesicles are observed throughout poliovirus infection, suggesting that infection induces a block to their maturation. These double membranes are known to acquire late endocytic markers such as LAMP-1, and the physical integrity of the ultrastructurally observed inner membrane is not known. Outside poliovirus-infected cells, small, single-membraned structures that contain virions and LC3 occasionally have been observed (27, 65).

What would be the advantage to a virus of anchoring its RNA replication complexes to the microtubule network of the cell? First, it is possible that the binding of the virus-induced vesicles to microtubules is incidental to the block in protein secretion induced by viral protein 3A. Although the role of microtubules in endoplasmic reticulum-to-Golgi traffic is a matter of some debate, it is possible that the roles of 3A protein in inhibiting protein transport and in LC3-containing vesicle immobilization are intertwined. Second, anchoring the autophagosome-like vesicles along the microtubule network may be a mechanism to prevent their maturation and fusion with lysosomes (18, 35). A similar block in autophagosome maturation was identified in *Legionella* (59); bacteria that replicate within membranes that bear autophagosomal markers secrete a factor that delays fusion with lysosomes and subsequent degradation (20). Finally, it may be important to control structures, such as double-membraned vesicles, that allow viral dissemination. Viral release by AWOL could be minimized during infection by tethering the vesicles to microtubules and then allowed when microtubules break down under natural circumstances such as the end of infection, the entry of the infected cell into mitosis, or a change in differentiation state. The mechanism by which poliovirus can exit cells in the absence of lysis, and the regulation of this mechanism, is likely to be relevant to other apparently nonlytic release events, such as the escape of other cytosolic microbes such as *Cryptococcus* and hepatitis A virus or the spread of aggregated cytoplasmic proteins through tissues.

ACKNOWLEDGMENTS

We thank Jennifer Ptacek, Peter Sarnow, and Michel Brahic for experimental suggestions and comments on the manuscript, Tim Stearns for advice on microtubule visualization, and Julie Theriot for guidance in tracking motile particles.

This work was supported by NIH training grant traineeships (M.P.T. and T.B.B.), the Advancing a Healthier Wisconsin program (W.T.J.), and an NIH Pioneer award (K.K.).

REFERENCES

1. **Alvarez, M., and A. Casadevall.** 2006. Phagosome extrusion and host-cell survival after Cryptococcus neoformans phagocytosis by macrophages. Curr. Biol. **16:**2161–2165.
2. **Bampton, E. T., C. G. Goemans, D. Niranjan, N. Mizushima, and A. M. Tolkovsky.** 2005. The dynamics of autophagy visualized in live cells: from autophagosome formation to fusion with endo/lysosomes. Autophagy **1:**23–36.
3. **Barco, A., and L. Carrasco.** 1995. A human virus protein, poliovirus protein 2BC, induces membrane proliferation and blocks the exocytic pathway in the yeast Saccharomyces cerevisiae. EMBO J. **14:**3349–3364.
4. **Bélanger, M., P. H. Rodrigues, W. A. Dunn, Jr., and A. Progulske-Fox.** 2006. Autophagy: a highway for Porphyromonas gingivalis in endothelial cells. Autophagy **2:**165–170.
5. **Belov, G. A., Q. Feng, K. Nikovics, C. L. Jackson, and E. Ehrenfeld.** 2008. A critical role of a cellular membrane traffic protein in poliovirus RNA replication. PLoS Pathog. **4:**e1000216.
6. **Berkova, Z., S. E. Crawford, G. Trugnan, T. Yoshimori, A. P. Morris, and M. K. Estes.** 2006. Rotavirus NSP4 induces a novel vesicular compartment regulated by calcium and associated with viroplasms. J. Virol. **80:**6061–6071.
7. **Berstein, H. D., and D. Baltimore.** 1988. Poliovirus mutant that contains a cold-sensitive defect in viral RNA synthesis. J. Virol. **62:**2922–2928.
8. **Bienz, K., D. Egger, Y. Rasser, and W. Bossart.** 1983. Intracellular distribution of poliovirus proteins and the induction of virus-specific cytoplasmic structures. Virology **131:**39–48.
9. **Bienz, K., D. Egger, and D. A. Wolff.** 1973. Virus replication, cytopathology, and lysosomal enzyme response of mitotic and interphase Hep-2 cells infected with poliovirus. J. Virol. **11:**565–574.
10. **Bilir, A., M. A. Altinoz, M. Erkan, V. Ozmen, and A. Aydiner.** 2001. Autophagy and nuclear changes in FM3A breast tumor cells after epirubicin, medroxyprogesterone and tamoxifen treatment in vitro. Pathobiology **69:**120–126.
11. **Bolten, R., D. Egger, R. Gosert, G. Schaub, L. Landmann, and K. Bienz.** 1998. Intracellular localization of poliovirus plus- and minus-strand RNA visualized by strand-specific fluorescent in situ hybridization. J. Virol. **72:**8578–8585.
12. **Cho, M. W., N. Teterina, D. Egger, K. Bienz, and E. Ehrenfeld.** 1994. Membrane rearrangement and vesicle induction by recombinant poliovirus 2C and 2BC in human cells. Virology **202:**129–145.
13. **Clayson, E. T., L. V. Brando, and R. W. Compans.** 1989. Release of simian virus 40 virions from epithelial cells is polarized and occurs without cell lysis. J. Virol. **63:**2278–2288.
14. **Dales, S., H. J. Eggers, I. Tamm, and G. E. Palade.** 1965. Electron microscopic study of the formation of poliovirus. Virology **26:**379–389.
15. **Dodd, D. A., T. H. Giddings, Jr., and K. Kirkegaard.** 2001. Poliovirus 3A protein limits interleukin-6 (IL-6), IL-8, and beta interferon secretion during viral infection. J. Virol. **75:**8158–8165.
16. **Doedens, J., L. A. Maynell, M. W. Klymkowsky, and K. Kirkegaard.** 1994. Secretory pathway function, but not cytoskeletal integrity, is required in poliovirus infection. Arch. Virol. Suppl. **9:**159–172.
17. **Ebina, T., M. Satake, and N. Ishida.** 1978. Involvement of microtubules in cytopathic effects of animal viruses: early proteins of adenovirus and herpesvirus inhibit formation of microtubular paracrystals in HeLa-S3 cells. J. Gen. Virol. **38:**535–548.
18. **Fass, E., E. Shvets, I. Degani, K. Hirschberg, and Z. Elazar.** 2006. Microtubules support production of starvation-induced autophagosomes but not their targeting and fusion with lysosomes. J. Biol. Chem. **281:**36303–36316.
19. **Feierbach, B., M. Bisher, J. Goodhouse, and L. W. Enquist.** 2007. In vitro analysis of transneuronal spread of an alphaherpesvirus infection in peripheral nervous system neurons. J. Virol. **81:**6846–6857.

20. **Fernandez-Moreira, E., J. H. Helbig, and M. S. Swanson.** 2006. Membrane vesicles shed by *Legionella pneumophila* inhibit fusion of phagosomes with lysosomes. Infect. Immun. **74:**3285–3295.
21. **Gauss-Müller, V., and F. Deinhardt.** 1984. Effect of hepatitis A virus infection on cell metabolism in vitro. Proc. Soc. Exp. Biol. Med. **175:**10–15.
22. **Giddings, T. H.** 2003. Freeze-substitution protocols for improved visualization of membranes in high-pressure frozen samples. J. Microsc. **212:**53–61.
23. **Hamano, T., T. F. Gendron, E. Causevic, S. H. Yen, W. L. Lin, C. Isidoro, M. Deture, and L. W. Ko.** 2008. Autophagic-lysosomal perturbation enhances tau aggregation in transfectants with induced wild-type tau expression. Eur. J. Neurosci. **27:**1119–1130.
24. **Hollinger, F. B., and J. Ticehurst.** 1990. Hepatitis A virus, p. 631–667. *In* B. N. Fields and D. M. Knipe (eds.), Fields virology, 2nd ed. Raven Press, New York, NY.
25. **Ichimura, Y., T. Kirisako, T. Takao, Y. Satomi, Y. Shimonishi, N. Ishihara, N. Mizushima, I. Tanida, E. Kominami, M. Ohsumi, T. Noda, and Y. Ohsumi.** 2000. A ubiquitin-like system mediates protein lipidation. Nature **408:**488–492.
26. **Iwata, A., B. E. Riley, J. A. Johnson, and R. R. Kopito.** 2005. HDAC6 and microtubules are required for autophagic degradation of aggregated huntington. J. Biol. Chem. **280:**40282–40292.
27. **Jackson, W. T., T. H. Giddings, Jr., M. P. Taylor, S. Mulinyawe, M. Rabinovitch, R. R. Kopito, and K. Kirkegaard.** 2005. Subversion of cellular autophagosomal machinery by RNA viruses. PLoS Biol. **3:**e156.
28. **Jahreiss, L., F. M. Menzies, and D. C. Rubinsztein.** 2008. The itinerary of autophagosomes: from peripheral formation to kiss-and-run fusion with lysosomes. Traffic **9:**574–587.
29. **Joachims, M., K. S. Harris, and D. Etchison.** 1995. Poliovirus protease 3C mediates cleavage of microtubule-associated protein 4. Virology **211:**451–461.
30. **Jourdan, N., M. Maurice, D. Delautier, A. M. Quero, A. L. Servin, and G. Trugnan.** 1997. Rotavirus is released from the apical surface of cultured human intestinal cells through nonconventional vesicular transport that bypasses the Golgi apparatus. J. Virol. **71:**8268–8278.
31. **Kim, J., and D. J. Klionsky.** 2000. Autophagy, cytoplasm-to-vacuole targeting pathway, and pexophagy in yeast and mammalian cells. Annu. Rev. Biochem. **69:**303–342.
32. **Kimura, S., T. Noda, and T. Yoshimori.** 2008. Dynein-dependent movement of autophagosomes mediates efficient encounters with lysosomes. Cell Struct. Funct. **33:**109–122.
33. **Kirkegaard, K., and W. T. Jackson.** 2005. Topology of double-membraned vesicles and the opportunity for non-lytic release of cytoplasm. Autophagy **1:**182–184.
34. **Klionsky, D. J.** 2005. The molecular machinery of autophagy: unanswered questions. J. Cell Sci. **118:**7–18.
35. **Köchl, R., X. W. Hu, E. Y. W. Chan, and S. Tooze.** 2006. Microtubules facilitate autophagosome formation and fusion of autophagosomes with endosomes. Traffic **7:**129–145.
36. **Kondratova, A. A., N. Neznanov, R. V. Kondratov, and A. V. Gudkov.** 2005. Poliovirus protein 3A binds and inactivates LIS1, causing block of membrane protein trafficking and deregulation of cell division. Cell Cycle **4:**1403–1410.
37. **Kuznetsov, S. A., and V. I. Gelfand.** 1987. 18 kDa microtubule-associated protein: identification as a new light chain (LC-3) of microtubule-associated protein 1 (MAP-1). FEBS Lett. **212:**145–148.
38. **Lee, Y. R., H. Y. Lei, M. T. Liu, J. R. Wang, S. H. Chen, Y. F. Jiang-Shieh, Y. S. Lin, T. M. Yeh, C. C. Liu, and H. S. Liu.** 2008. Autophagic machinery activated by dengue virus enhances virus replication. Virology **374:**240–248.
39. **Lenk, R., and S. Penman.** 1979. The cytoskeletal framework and poliovirus metabolism. Cell **16:**289–301.
40. **Levine, B., and D. J. Klionsky.** 2004. Development by self-digestion: molecular mechanisms and biological functions of autophagy. Dev. Cell **6:**463–477.
41. **Lloyd, R. E., and M. Bovee.** 1993. Persistent infection of human erythroblastoid cells by poliovirus. Virology **194:**200–209.
42. **Lyman, M. G., B. Feierbach, D. Curanovic, M. Bisher, and L. W. Enquist.** 2007. Pseudorabies virus Us9 directs axonal sorting of viral capsids. J. Virol. **81:**11363–11371.
43. **Mizushima, N., B. Levine, A. M. Cuervo, and D. J. Klionsky.** 2008. Autophagy fights disease through cellular self-digestion. Nature **451:**1069–1075.
44. **Mizushima, N., Y. Ohsumi, and T. Yoshimori.** 2002. Autophagosome formation in mammalian cells. Cell Struct. Funct. **27:**421–429.
45. **Morrison, M. E., Y. J. He, M. W. Wien, J. M. Hogle, and V. R. Racaniello.** 1994. Homolog-scanning mutagenesis reveals poliovirus receptor residues important for virus binding and replication. J. Virol. **68:**2578–2588.
46. **Pelletier, I., G. Duncan, and F. Colbere-Garapin.** 1998. One amino acid change on the capsid surface of poliovirus sabin 1 allows the establishment of persistent infections in HEp-2c cell cultures. Virology **241:**1–13.
47. **Racaniello, V. R., and D. Baltimore.** 1981. Cloned poliovirus complementary DNA is infectious in mammalian cells. Science **214:**916–919.
48. **Ramanathan, H. N., D. H. Chung, S. J. Plane, E. Sztul, Y. K. Chu, M. C. Guttieri, M. McDowell, G. Ali, and C. B. Jonsson.** 2007. Dynein-dependent transport of the hantaan virus nucleocapsid protein to the endoplasmic reticulum-Golgi intermediate compartment. J. Virol. **81:**8634–8647.
49. **Ravikumar, B., A. Acevedo-Arozena, S. Imarisio, Z. Berger, C. Vacher, C. J. O'Kane, S. D. Brown, and D. C. Rubinsztein.** 2005. Dynein mutations impair autophagic clearance of aggregate-prone proteins. Nat. Genet. **37:**771–776.
50. **Ravikumar, B., C. Vacher, Z. Berger, J. E. Davies, S. Luo, L. G. Oroz, F. Scaravilli, D. F. Easton, R. Duden, C. J. O'Kane, and D. C. Rubinsztein.** 2004. Inhibition of mTOR induces autophagy and reduces toxicity of polyglutamine expansions in fly and mouse models of Huntington disease. Nat. Genet. **36:**585–595.
51. **Ren, P. H., J. E. Lauckner, I. Kachirskaia, J. E. Heuser, R. Melki, and R. R. Kopito.** 2009. Cytoplasmic penetration and persistent infection of mammalian cells by polyglutamine aggregates. Nat. Cell Biol. **11:**219–225.
52. **Rothe, J., W. Lesslauer, H. Lotscher, Y. Lang, P. Koebel, F. Kontgen, A. Althage, R. M. Zinkernagel, M. Steinmetz, and H. Bluethmann.** 1993. Mice lacking the tumour necrosis factor receptor 1 are resistant to TNF-mediated toxicity but highly susceptible to infection by Listeria monocytogenes. Nature **364:**798–802.
53. **Roussarie, J. P., C. Ruffie, J. M. Edgar, I. Griffiths, and M. Brahic.** 2007. Axon myelin transfer of a non-enveloped virus. PLoS One **2:**e1331.
54. **Schlegel, A., T. H. Giddings, Jr., M. S. Ladinsky, and K. Kirkegaard.** 1996. Cellular origin and ultrastructure of membranes induced during poliovirus infection. J. Virol. **70:**6576–6588.
55. **Smith, D. S., M. Niethammer, R. Ayala, Y. Zhou, M. J. Gambello, A. Wynshaw-Boris, and L. H. Tsai.** 2000. Regulation of cytoplasmic dynein behaviour and microtubule organization by mammalian Lis1. Nat. Cell Biol. **2:**767–775.
56. **Smith, G. L., and M. Law.** 2004. The exit of vaccinia virus from infected cells. Virus Res. **106:**189–197.
57. **Strauss, D. M., L. W. Glustrom, and D. S. Wuttke.** 2003. Towards an understanding of the poliovirus replication complex: the solution structure of the soluble domain of the poliovirus 3A protein. J. Mol. Biol. **330:**225–234.
58. **Suhy, D. A., T. H. Giddings, Jr., and K. Kirkegaard.** 2000. Remodeling the endoplasmic reticulum by poliovirus infection and by individual viral proteins: an autophagy-like origin for virus-induced vesicles. J. Virol. **74:**8953–8965.
59. **Swanson, M. S., and R. R. Isberg.** 1996. Identification of *Legionella pneumophila* mutants that have aberrant intracellular fates. Infect. Immun. **64:**2585–2594.
60. **Tanida, I., Y. S. Sou, J. Ezaki, N. Minematsu-Ikeguchi, T. Ueno, and E. Kominami.** 2004. HsAtg4B/HsApg4B/autophagin-1 cleaves the carboxyl termini of three human Atg8 homologues and delipidates microtubule-associated protein light chain 3- and GABAA receptor-associated protein-phospholipid conjugates. J. Biol. Chem. **279:**36268–36276.
61. **Taylor, M. P., and K. Kirkegaard.** 2007. Modification of cellular autophagy protein LC3 by poliovirus. J. Virol. **81:**12543–12553.
62. **Taylor, M. P., and K. Kirkegaard.** 2008. Potential subversion of autophagosomal pathway by picornaviruses. Autophagy **4:**286–289.
63. **Teterina, N. L., A. E. Gorbalenya, D. Egger, K. Bienz, and E. Ehrenfeld.** 1997. Poliovirus 2C protein determinants of membrane binding and rearrangements in mammalian cells. J. Virol. **71:**8962–8972.
64. **Towner, J., and B. L. Semler.** 1996. Determinants of membrane association on poliovirus protein 3AB. J. Biol. Chem. **271:**26810–26818.
65. **Tucker, S. P., C. L. Thornton, E. Wimmer, and R. W. Compans.** 1993. Vectorial release of poliovirus from polarized human intestinal epithelial cells. J. Virol. **67:**4274–4282.
66. **Vogiatzi, T., M. Xilouri, K. Vekrellis, and L. Stefanis.** 2008. Wild type alpha-synuclein is degraded by chaperone-mediated autophagy and macroautophagy in neuronal cells. J. Biol. Chem. **283:**23542–23556.